AIP Journal of Applied Physics

Modelling a point absorbing wave energy converter by the equivalent electric circuit theory: A feasibility study

Ling Hai, Olle Svensson, Jan Isberg, and Mats Leijon

Citation: Journal of Applied Physics **117**, 164901 (2015); doi: 10.1063/1.4918903
View online: http://dx.doi.org/10.1063/1.4918903
View Table of Contents: http://scitation.aip.org/content/aip/journal/jap/117/16?ver=pdfcov
Published by the AIP Publishing

Modelling a point absorbing wave energy converter by the equivalent electric circuit theory: A feasibility study

Ling Hai,[1,a)] Olle Svensson,[1] Jan Isberg,[1] and Mats Leijon[1,2]
[1]*Department of Engineering Sciences, Swedish Centre for Renewable Electric Energy Conversion, Division of Electricity, Ångström Laboratory, Uppsala University, Box 534, 75121 Uppsala, Sweden*
[2]*Faculty of Engineering and the Environment, Energy and Climate Change Division, University of Southampton, Southampton, United Kingdom*

(Received 6 March 2015; accepted 10 April 2015; published online 22 April 2015)

There is a need to have a reliable tool to quickly assess wave energy converters (WECs). This paper explores whether it is possible to apply the equivalent electric circuit theory as an evaluation tool for point absorbing WEC system modelling. The circuits were developed starting from the force analysis, in which the hydrodynamic, mechanical, and electrical parameters were expressed by electrical components. A methodology on how to determine the parameters for electrical components has been explained. It is found that by using a multimeter, forces in the connection line and the absorbed electric power can be simulated and read directly from the electric circuit model. Finally, the circuit model has been validated against the full scale offshore experiment. The results indicated that the captured power could be predicted rather accurately and the line force could be estimated accurately near the designed working condition of the WEC. [http://dx.doi.org/10.1063/1.4918903]

I. INTRODUCTION

Ocean wave energy has gained considerable attention as a type of abundant, enduring, and predictable renewable energy source. It has been proven that wave energy can be harnessed and converted into electrical energy using different methods.[1,2] A point absorbing wave energy converter (WEC) illustrated in Fig. 1(a) is a typical example of a device invented for this purpose. The WEC unit consists of a floating buoy on the water surface, a connection line, and a linear synchronous generator. When the buoy moves up and down with the waves, it drags the translator inside the generator to move as well. The translator's vertical motion creates a changing magnetic field, which will induce a voltage in the stator windings. In this context, the size of the buoy is smaller than the wavelengths of the incident waves, which is why it is called a point absorber.

For point absorbing WECs, the geometry and dimension of the floating buoy heavily influence the energy absorption. Moreover, the match between the buoy and the electromagnetic damping level is crucial for economic and technical reasons. Therefore, in addition to the modelling of the hydrodynamic performance of the buoy and the Power Take-Off (PTO) system on their own, a system modelling is also needed. PTO refers to the method of extracting energy from an energy source. Common PTO systems in wave energy field are hydraulic, pneumatic, or electric. The PTO system discussed in this paper is confined to a linear generator using all-electric conversion.[3]

To make system modelling more efficient and less complicated, one solution is to create a common language for modelling. This paper tries to utilize the electric circuit as a bridge to connect the hydrodynamics and PTO system. An RLC series electric circuit has been used for modelling the relations between the different parts of a point absorbing WEC. The idea of employing equivalent circuit technique for WEC system modelling is not new; many have used the linearized circuit model to improve the understanding of the WEC system, two typical examples are Refs. 4 and 5. It has also been applied in the control strategy study which aims for an optimum power extraction, such as Refs. 6–9. To the best knowledge of the authors, there is no non-linear equivalent circuit model established for actual point absorbing WEC system, for the existed linearized model, its accuracy has not been examined thoroughly, nor the methodology of applying such models on the WEC design has been addressed. Therefore, the paper will study on these aspects in detail.

The electric power output generated by the linear generator and the peak force in the connection line are the two key parameters when it comes to the design and evaluation of a WEC. The former is essential for its decisive influence on economic profit, the latter is closely related to the cost: it determines how strong a generator and how heavy a concrete platform need to be. Therefore, the equivalent electric circuit model will be applied to mainly evaluate these two parameters.

II. COMPLETE ELECTRIC CIRCUIT MODEL

A. Force analysis of a WEC system

There are six degrees of freedom for a floating buoy, however, only the heave motion will be considered here

[a)]Author to whom correspondence should be addressed. Electronic mail: Ling.Hai@angstrom.uu.se. Tel.: +46(0)18471 5870. Fax: +46(0)18471 5810.

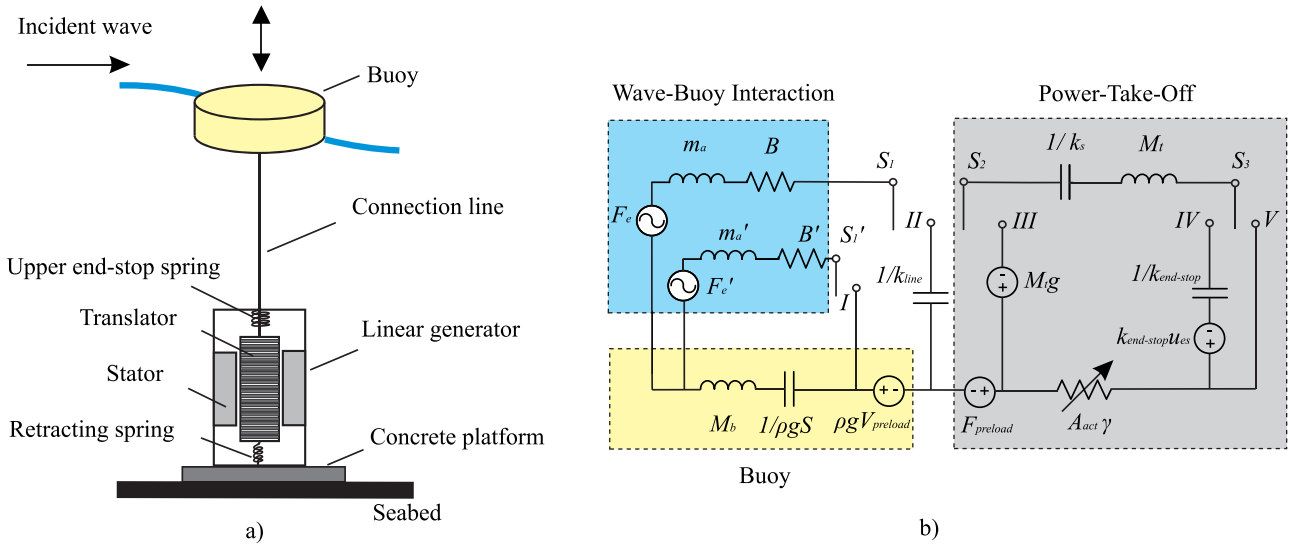

FIG. 1. (a) Sketch of the principle and design of the WEC. (b) The complete equivalent electric circuit model for (a).

since other motions have been proven to have no significant impact on the line force.[10]

In general, the motion of the WEC model can be described by two differential equations:

$$M_b\ddot{z}_b(t) = F_e(t) - F_r(t) - \rho g S z_b(t) - F_{line}, \tag{1}$$

$$M_t\ddot{z}_t(t) = F_{line} - F_{end-stop} - F_s - F_{PTO} + F_{mg}. \tag{2}$$

Here, the subscript b denotes the buoy, and subscript t denotes the translator. M is the mass, $z(t)$ is the vertical displacement from the equilibrium position, $\dot{z}(t)$ and $\ddot{z}(t)$ are the velocity and acceleration, respectively. $\rho g S z_b(t)$ entails the variable part of the hydrostatic force of the buoy caused by the deviation from the equilibrium position. The former design of the generators has a retracting spring to adjust the draft of the buoy, which brings a spring force F_s into the system, for later generators that have no retracting springs, this term will be eliminated.

The excitation force and radiation force are normally calculated in the frequency domain first

$$F_e(\omega) = f_e(\omega)\eta(\omega), \tag{3}$$

$$F_r(\omega) = [i\omega m_a(\omega) - B(\omega)]\dot{z}(\omega). \tag{4}$$

Then, they can be calculated in the time domain by

$$F_e(t) = f_e(t) * \eta(t), \tag{5}$$

$$F_r(t) = m_a(\infty)\ddot{z}(t) + \int_0^\infty L(\tau)\ddot{z}(t-\tau)d\tau. \tag{6}$$

In Eq. (4), $m_a(\omega)$ is the added mass, which means the surrounding water oscillating together with the buoy. $B(\omega)$ is the radiation damping coefficient. In Eq. (5), the single asterisk $*$ represents the convolution operation. $L(t)$ in Eq. (6) could be calculated by either Eq. (7) or Eq. (8).[11]

$$L(t) = \frac{2}{\pi}\int_0^\infty [m_a(\omega) - m_a(\infty)]\cos\omega t d\omega \tag{7}$$

or

$$L(t) = \frac{2}{\pi}\int_0^\infty \frac{B(\omega)}{\omega}\sin\omega t d\omega. \tag{8}$$

F_{line} is the force in the connection line, which can be modelled as a very stiff spring with a spring constant of k_{line}, the line force becomes 0 if the line is slack

$$F_{line} = \begin{cases} k_{line}(z_b - z_t) & \text{if } z_b > z_t \\ 0 & \text{else.} \end{cases} \tag{9}$$

$F_{end-stop}$ is the force that results from the compression of the upper or lower end-stop springs when the translator hits the end-stop springs. In the sketch in Fig. 1(a), only the upper end-stop spring is drawn. In real life, however, a generator will normally have end-stop springs on both sides to protect the translator and the hall structure from large waves.

The spring force from the retracting spring includes static preload force and dynamic spring force when the line is tightened. The preload force will disappear once the line is slack. Here, the k_s is the spring constant of the retracting spring

$$F_s = \begin{cases} k_s z_t + F_{preload} & \text{if } z_b > z_t \\ k_s z_t & \text{else.} \end{cases} \tag{10}$$

F_{PTO} is the electromagnetic damping force from the PTO mechanism. It can be calculated via Eq. (11), in which γ is the electromagnetic damping coefficient, A_{act} is a ratio ranging from 0 to 1, which describes the extent of active overlapping between the stator and the translator.

$$F_{PTO} = A_{act}\gamma\dot{z}_t(t). \tag{11}$$

F_{mg} equals the gravity force of the translator when the connection line is slack. It will be balanced by the buoyancy force from the buoy if the line is lifting the translator, i.e., when the line force is bigger than zero.

$$F_{mg} = \begin{cases} 0 & \text{if } z_b > z_t \\ M_t g & \text{else.} \end{cases} \quad (12)$$

B. Circuit diagram

On the basis of the force analysis and an enumeration of all possible situations a WEC might undergo, an equivalent electric circuit has been derived, as illustrated in Fig. 1(b). In the electric circuit model, the excitation force F_e is the driving force, and can thus be modelled as the voltage source. The velocity $\dot{z}$ performs as the current in an electric circuit. It is worth mentioning that the DC voltage source $F_{preload}$ on the translator side and the corresponding buoyancy force that is caused by the preload spring force $\rho g V_{preload}$ on the buoy side are equal in magnitude but opposite in directions.

The equivalent electric circuit is composed of three parts: the hydrodynamic interaction between the incident waves and the floating buoy, the physical parameters of the buoy, and the mechanical and electrical damping of the PTO mechanism. The mechanical losses of the system are neglected here.

The model could simulate different situations by switching circuit switches to different positions: S_1' and S_1 can be connected to positions *I* and *II*, respectively, which are correspondent to the buoy is moving without or with tension in the line. In the graph, the prime symbol $'$ indicates the status that the line is slack while the buoy is floating freely. The hydrodynamic parameters under this circumstance need to be calculated with respect to the decreased draft of the buoy, which is resulted from the absence of the translator weight. S_2 can be connected to positions *II* and *III*, which are correspondent to the translator is lifted by the connection line or drops under its gravity force. Switch S_3 can be connected with positions *IV* and *V*, depending on if the translator hits the end-stop spring or not.

A WEC will undergo many different conditions while operating in the ocean. It could run smoothly when the wave is moderate, or barely move during small waves. It may perform in a disruptive manner during storms. To explain the different conditions in a concise way, we take a big wave as an example—assuming all the possible conditions that may happen to the WEC system within a wave cycle—to illustrate how the generated power and force in the connection line would behave. Fig. 2 demonstrates the translator position, the force in the connection line, and the instantaneous output power during this wave cycle. In the translator position graph, u_{es} and u_{lim} denoted the distance from top of the translator to the upper end-stop spring when the spring was not compressed at all, or had been compressed to its limit. Likewise, b_{es} and b_{lim} meant the distance from the bottom of the translator to the bottom end-stop spring when it was not compressed or was fully compressed. Table I provides explanations on how to link the electric circuit model layout with the different status shown in Fig. 2.

As mentioned, Fig. 2 and Table I summarise all the possible conditions in one wave cycle. The example can be taken as a basis for the analysis, while the real situation may alter for different tides, waves, and WEC configurations. For instance, small waves will seldom have the translator hitting the upper end-stop spring, so the conditions happening during t_1–t_4 might not appear.

C. A short discussion

The analysis shown in Fig. 2 pointed out that most of the power is generated when the translator does not hit the end-stop spring, at the so called "free stroke length" interval. Unwanted peak line force and low power production appear at the region where the translator hits the end-stop spring. This hypothesis has been confirmed from offshore experimental results presented in Refs. 12 and 13. Therefore, it will be efficient to look into the period where the translator is moving freely without bumping into the end-stop spring, to get a rough estimation of the output power and the peak force in the line.

III. SIMPLIFIED ELECTRIC CIRCUIT MODEL

A. Force analysis for a linear WEC system

A simple model can be established if a WEC worked in a linear manner. In this case, four conditions need to be fulfilled: first, the buoy is semi-submerged in a linear potential flow of an ideal incompressible liquid; second, the stiff connection line is always tightened without being slack or elastic; third, the translator moves within the stroke length region where the end-stop springs are not compressed, and last the stator is always fully active, i.e., A_{act} equals to 1. For a linear WEC system, the buoy and the translator can be regarded as one piece since they are moving together. The motion equation is therefore simplified to,

$$(M_b + M_t)\ddot{z}(t) = F_e(t) - F_r(t) - (\rho g S + k_s) z(t) - \gamma \dot{z}(t). \quad (13)$$

Here, $z(t)$ is the vertical displacement with respect to the individual equilibrium positions for the buoy and translator. In frequency domain, the equation becomes

$$-\omega^2 [M_b + M_t + m_a(\omega)] z(\omega) = f_e(\omega)\eta(\omega) - (\rho g S + k_s) z(\omega) - i\omega[\gamma + B(\omega)] z(\omega). \quad (14)$$

B. Circuit diagram: The application

An RLC series electric circuit presented in Fig. 3 has been drawn according to Eq. (14), it will be more explicit if we formulate the equation as

$$f_e(\omega)\eta(\omega) = \left[i\omega(M_b + M_t + m_a(\omega)) + \frac{\rho g S + k_s}{i\omega} + \gamma + B(\omega) \right] i\omega z(\omega). \quad (15)$$

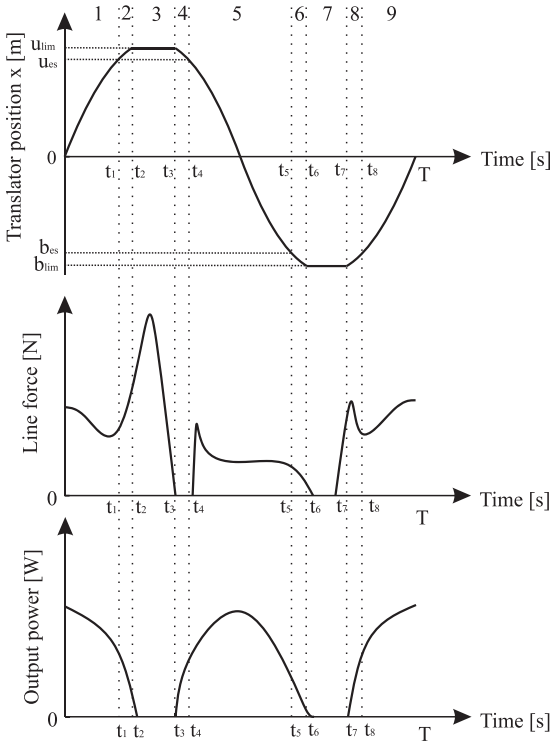

FIG. 2. Sketch of all the possible conditions of a WEC.

This circuit is one case of the complete electric circuit, when the switches S_1 and S_2 are connected to position *II* and the switch S_3 is connected with position *V*. The stiff connection line is analogous to an open circuit since k_{line} goes to infinite, which leads to an infinitely big impedance of the capacitor. One voltage meter, whose internal impedance is infinite, has been placed at the former capacitor place to indicate how the line force can be measured. An ampere meter has been placed in the circuit to measure the velocity of the buoy or the translator.

From the equivalent electric circuit model, the electromagnetic damping coefficient γ is a resistor and the translator velocity is the current. Therefore, simply by reading the power consumption on resistor γ, we could know how much active power has been absorbed by the system

$$P_{PTO} = F_{PTO} v = \gamma \dot{z}^2. \tag{16}$$

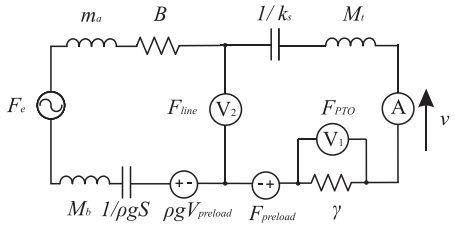

FIG. 3. Simplified electric circuit model for a linear WEC system.

The physical meaning of the stiff line force here only refers to the internal stress force of the line when one looks into its cross-sectional area. The line does not get elongated itself or contribute any elastic force any more. To measure the internal force existing in the connection line, one can start from a force analysis of either the translator or the buoy. If looked into the translator side, the force can be written as

$$F_{line} = j\omega z(\omega)\left[(j\omega M_t) + \gamma + \frac{1}{j\omega\frac{1}{k_s}}\right] + F_{preload}. \tag{17}$$

Since $j\omega z(\omega) = v(\omega)$ is the velocity, it implies that the force in the line can be read from the voltage drop over the inductor M_t, resistor γ, and capacitor $\frac{1}{k_s}$ in the circuit model, as the voltage meter V_2 measures in Fig. 3

$$F_{line} = U_{M_t} + U_\gamma + U_{\frac{1}{k_s}} + U_{preload}. \tag{18}$$

C. Method to determine the circuit parameters

The equivalent electric circuit model contains certain components that are fixed in value: the capacitors $1/k_s$ and $1/\rho gS$, the inductors M_t and M_b. Other components such as the voltage source F_e, inductor m_a, resistor B, and γ will vary with different sea states.

Assume a monochromatic sinusoidal wave with a height of H_s and a period of T_e is the incoming wave. Since the WEC moves linearly, it implies that the buoy will follow the incoming wave and oscillates with the same frequency $f = 1/T_e$ and amplitude $A = \frac{1}{2}H_s$. The hydrodynamic coefficients f_e, m_a, and B for per unit length over certain range of frequency could be computed from the commercial code

TABLE I. Possible status of the WEC and the equivalent electric circuit layout.

No.	Time interval	Connection of switches	System status
1	$0 - t_1$	$S_1 - II, S_2 - II, S_3 - V$	Translator goes up
2	$t_1 - t_2$	$S1 - II, S_2 - II, S_3 - IV$	Translator hits upper end-stop spring and continues rising
3	$t_2 - t_3$	$S_1 - II, (S_2)$[a], $S_3 - IV$	Translator stops moving, buoy undergoes lifting force from waves
4	$t_3 - t_4$	$S_1' - I, S_2 - III, S_3 - IV$	Buoy falls faster than translator, connection line is loose for a moment
5	$t_4 - t_5$	$S_1 - II, S_2 - II, S_3 - V$	Translator goes down, connection line is tighten[b]
6	$t_5 - t_6$	$S_1 - II, S_2 - II, S_3 - IV$	Translator hits the bottom end-stop spring and continues to fall
7	$t_6 - t_7$	$S_1' - I, S_2 - III, S_3 - IV$	Translator sits at the bottom, connection line is loose
8	$t_7 - t_8$	$S_1 - II, S_2 - II, S_3 - IV$	Translator goes up, lower end-stop spring is still compressed[b]
9	$t_8 - T$	$S_1 - II, S_2 - II, S_3 - V$	Translator goes up

[a]The bracket () means disconnection status, translator is constrained by mechanical limit in this case.
[b]The abrupt increase of the line force will not occur if the connection line is tight at the former status.

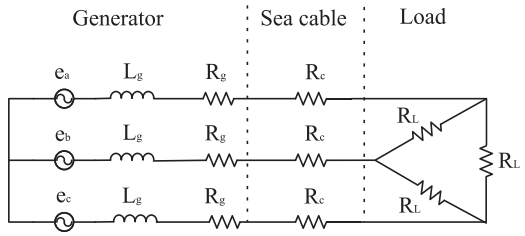

FIG. 4. Diagram of the equivalent PTO mechanism.

WAMIT,[14] the respective values for this specific sine wave can be calculated in Matlab, for instance, the amplitude of the AC voltage source F_e will be $|F_e|_{max} = f_e A$.

The basic electric circuit diagram of a generator connected with 3 identical resistive loads is presented in Fig. 4.[15] In the diagram, $e_{a,b,c}$ is the no load voltage of the generator, L_g is the generator inductance, R_g, R_c, and R_L are the resistances of the generator, sea cable, and load. The electromagnetic damping coefficient γ for different resistive loads has been previously simulated in Ref. 16 based on

$$\gamma = 3\left(\frac{1}{R_g}\left(\frac{V_g}{\dot{z}}\right)^2 + \frac{1}{R_c}\left(\frac{V_c}{\dot{z}}\right)^2 + \frac{1}{R_L}\left(\frac{V_L}{\dot{z}}\right)^2\right), \tag{19}$$

where the V_g, V_c, and V_L are the effective voltage drops over the R_g, R_c, and R_L. The damping coefficient γ differs for different translator speed and load. To simplify the model one step further, a constant γ at the rated speed for 2.2 Ω resistive load has been trialled in the validation.

So far, all the parameters in the circuit model can been determined. The average power and the peak line force are of more interest when it comes to the evaluation of the WEC, since a total electric energy production correlates highly with the average power instead of the maximum power, while knowing the peak force, even only under medium or small waves, is essential for determining the nominal capacity and fatigue problem of mechanical parts. The average absorbed power over one wave period is half of the maximum power if the wave is sinusoidal:

$$P_{avg} = \frac{1}{2}P_{max}. \tag{20}$$

D. Experimental verification

To validate the simplified equivalent electric circuit model, experimental data collected from a full scale offshore test have been examined. The data include both the captured electric power and line force measurement results; they were collected between 2007-03-08 and 2007-03-14. The experiment took place at Swedish west coast, close to a town named Lysekil. The water depth at the test site is around 25 m, and the major configuration of the WEC has been listed in Table II.

The total captured active power by the WEC includes the electric power consumed by the resistive load P_{load}, and the power losses in the generator $P_{generator}$ and sea cable P_{cable}

TABLE II. Main features of the WEC.[16]

Buoy radius	a	1.5 m
Buoy height	h_b	0.8 m
Draft	b	0.4 m
Buoy weight	M_b	1000 kg
Rated power	P_r	10 kW
Rated speed	v_r	0.67 m/s
Translator weight	M_t	1000 kg
Retracting spring constant	k_s	6.2 kN/m
Initial spring retracting force at equilibrium position	$F_{preload}$	8.12 kN
Generator resistance	R_g	0.45Ω
Generator inductance	L_g	5.5 mH
Sea cable resistance	R_c	0.5 Ω
Load resistance	R_L	2.2 Ω

$$P_{captured} = P_{generator} + P_{cable} + P_{load}. \tag{21}$$

An example has been given in Fig. 5 illustrating how the experimental data over 10 min get processed. The average total captured power is taken from counting the average of all the measured power values, which has been marked as the red horizontal line in Fig. 5(a). The average peak force

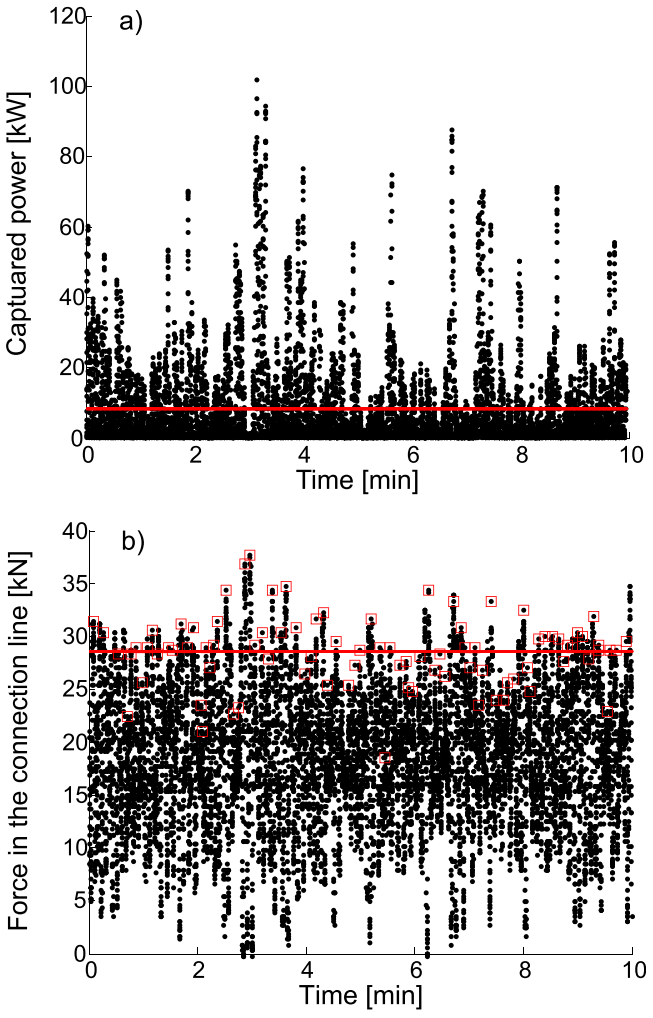

FIG. 5. An example of 10 min measured (a) captured power. (b) Peak force in the connection line.

during this 10 min is calculated by counting the mean value of the peak force for each cycle, and is marked as the red horizontal line as well in Fig. 5(b).

From the 10 min sea states during which experimental data are gathered, the significant wave height and energy period could be calculated. Using the monochromatic sinusoidal wave defined by these two parameters and applying the method provided in Subsection III C, one could obtain the circuit parameters for the simplified equivalent circuit model. The simulated results are ought to be measured when the circuit generates stable outputs.

E. Results

The experimental results for approximately 140 sea states have been analysed. Fig. 6(a) shows that the investigated data were measured when the significant wave climate height was between 0.3 m and 2.7 m, the wave energy period was between 4.3 s and 6.9 s, and the energy flux is mainly gathered between 1 kW/m and 24 kW/m. The wave climate is selected to cover the majority wave climate that may occur in Lysekil test site.[17]

Fig. 6(b) compares the average value of the captured electric power obtained from the experiments and the simplified equivalent electric circuit model. The blue circular dots represent the experimental results, while the red squares represent the results from the simulation model. Here, each experimental result is an average of the 10 min measurement, and each simulated result is measured as the average absorbed power on resistor γ when the circuit has a stable output.

The peak line force has been compared in a similar way, as displayed in Fig. 6(c). One blue circular dot means an average of the 10 min measured peak line force, and one red square means the maximum voltage V_2 read from the circuit simulation when the circuit is stable.

The trend lines in Figs. 6(b) and 6(c) are the polynomials of order 3. It is to make a more intuitive comparison between two groups of the scattered data.

IV. DISCUSSIONS

The concept of expressing the point absorbing WEC system by an equivalent electric circuit has been thoroughly investigated. The principle is to follow the force analysis, through which the velocity can be modelled as the current, the force can be modelled as the voltage, and different WEC operational conditions correspond to the different circuit network layout that can be accomplished by changing the switch connections, as presented in Fig. 1(b).

In Sec. II, the work is focused on establishing a complete equivalent electric circuit model, and assessing its usability for the fast WEC system modelling. The analysis of using this model for one typical example in Fig. 2 demonstrated that the non-linear phenomena such as the snatch load forces, mechanical damping by end-stop springs, or the change of the active area ratio can be simulated via this electric analogue. Due to the fact that this circuit model is derived from a comprehensive force analysis, a good precision can be expected if the applications were for the transient

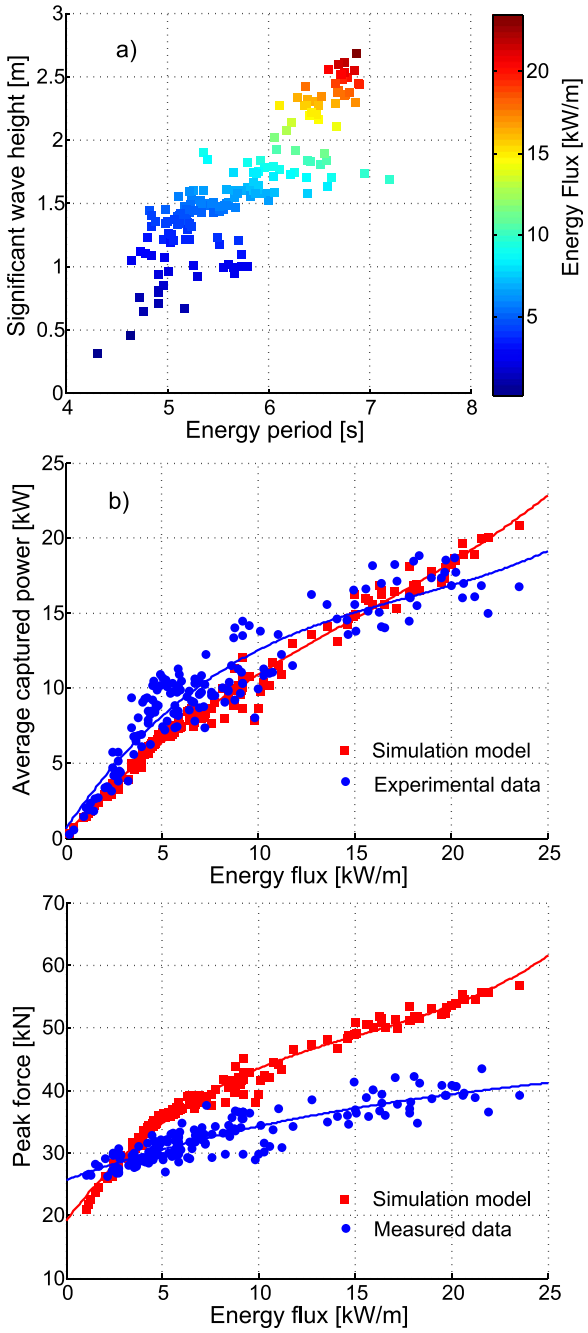

FIG. 6. (a) Wave climate of the investigated data. (b) Comparison of the captured electric power from experiments and circuit model. (c) Comparison of the peak line force from experiments and circuit model.

dynamic system analysis, or the real-time control strategy study, etc. While apparently the logic control is needed for the switches, it limits the potential of using this circuit as a simple simulation interface that everyone could make use of.

Hence, a simplified electric equivalence was studied at Sec. III. It targeted a narrower scope, which only includes an ideal WEC working under ideal sea states, no mechanical losses, nor the extreme weather conditions are considered in this case, which is the context when one started to design and adjust a WEC from scratch.

The results in Figs. 6(b) and 6(c) present both the simulated and experimental data of the power and force. A further calculation on the absolute difference has been given in Fig. 7.

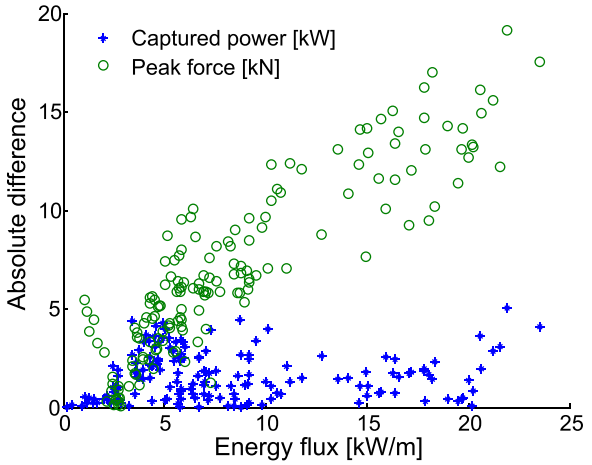

FIG. 7. The absolute difference of the average power and peak line force.

Both the average power and peak force predictions follow the experimental results at a glance, and the power has a better fitting compared with the force. The fluctuations have been anticipated since the electric circuit is derived from the linear force model and most non-linear facts have been omitted; one example is that the constant electromagnetic damping was evaluated when the translator moves with a speed of 0.67 m/s; this simplification could explain why the data fit better around the designed working region 5–8 kW/s, and tend to deviate more outside of the region. At last, the experimental data are statistical data representing the 10 min average; their accuracy can be limited by the measurement technique, like the sampling frequency, which would especially cause a bigger margin of error for the peak value compared with the average value.

Aside from the common sources of error analysed above, more information have been revealed from the results of the peak line force. The peak line force has been overestimated in the simulation when the wave energy flux is bigger than 5 kW/m, and the deviation grows proportionally to the wave energy flux: the bigger the waves are, the bigger the errors become. For wave flux more than 10 kW/m, the simulated peak force is around 10 kN bigger than the experimental results, i.e., 30% from the measured average value. One possible reason is that for big waves, if the buoy is fully submerged already and mechanically constrained within its stroke length, the excitation force will not be as big as if the buoy was freely oscillating in the wave: there will be water on the buoy which gives extra gravity force downwards. Another reason could be that we neglect the elastic force from the deformation of the connection line: the simplified model has taken the line as a stiff line having zero elasticity, therefore, when big waves happened, the model would count a bigger internal force, which in reality equals to the real internal force plus the elastic force from the connection line. Nevertheless, more studies are needed to investigate the line status for large waves to have a solid conclusion.

The simplified equivalent electric circuit model can be seen as the core of a WEC containing the most important parameters. Similar like Lego, it can be extended depending on the WEC mechanical design or the purpose of the study. The complete equivalent electric circuit can be seen as an intermediate version of the modelling that includes the major aspects. It still has spaces for extension if more factors were considered, for instance, this paper only introduced the passive loading situation, i.e., in the absence of the reactive component of PTO and F_{PTO} is linearly related with the velocity $\dot{z}_t$. If a WEC system used reactive or latching control strategies, the electromagnetic damping of the generator can be analogous in a more general form as a variable complex impedance $Z_{PTO} = R_{PTO} + jX_{PTO}$ in the equivalent circuit model. A thorough review on different electrical damping methods has been presented in Ref. 3 regarding this subject.

It is also worth mentioning that both electric circuit models proposed in this paper are supposed to be used when a potential linear wave theory is valid. This means that the non-linear wave hydrodynamic problems, e.g., steep waves, or the buoy encountered an over-topping situation, cannot be simulated via these two models.

Last but not least, the method of using the equivalent circuit theory for the WEC modelling has provided another perspective on understanding how each element in the WEC system interacts with each other, and their impacts to the whole WEC unit: first, the mass which includes the moving part and associated added mass is inductive: the higher the mass is, the higher inertia it will bring to the system. Second, the hydrostatic stiffness and the springs are capacitive, they represent the ability of storing potential energy in the oscillation process. A bigger water plane area of the buoy and spring constant will result in larger capacitive impedance in the circuit; therefore, more potential energy will be stored when the displacement was the same. Finally, in the entire energy conversion process, only the wave radiation damping and electromagnetic damping of the PTO consume the energy, other factors or components just introduce phase shifts between the velocity and the force, yet not consume any energy.

V. CONCLUSION

Being the first attempt of applying the equivalent electric circuit theory for a WEC system evaluation, this paper presented one complete and one simple electric circuit models. The complete circuit model is feasible to simulate different status of an actual point absorbing WEC operation, and the simple circuit model is considered more suitable if one wants a quick assessment. The verification for the simple model has revealed that a good prediction for the average captured electric power can be expected from this model, while the peak force in the connection line could be estimated reasonably only around the design working sea states. The validation also confirms that former studies using the simplified electric circuit model in control strategy design are reasonable. This research could benefit the early stage design of the WEC, especially for the size and geometry of the buoy, electromagnetic damping level, and the integration issues.

ACKNOWLEDGMENTS

The authors would like to thank the financial support from Vetenskapsrådet, Swedish Energy Agency, Swedish Research Council Grant Nos. KOF11 2011-6312 and 621-

2009-3417 for the project. The first author also wants to thank Dr. Jens Engström for the tutorials on using WAMIT software.

[1]A. F. de O. Falcão, "Wave energy utilization: A review of the technologies," Renewable Sustainable Energy Rev. **14**, 899–918 (2010).
[2]B. Drew, A. Plummer, and M. N. Sahinkaya, "A review of wave energy converter technology," Proc. Inst. Mech. Eng., Part A **223**, 887–902 (2009).
[3]R. Ekström, B. Ekergård, and M. Leijon, "Electrical damping of linear generators for wave energy convertersa review," Renewable Sustainable Energy Rev. **42**, 116–128 (2015).
[4]J. Shek, D. Macpherson, M. Mueller, and J. Xiang, "Reaction force control of a linear electrical generator for direct drive wave energy conversion," IET Renewable Power Gener. **1**, 17–24 (2007).
[5]T. Brekken, A. Jouanne, and H.-Y. Han, "Ocean wave energy overview and research at oregon state university," in *IEEE Proceedings on Power Electronics and Machines in Wind Applications, 2009, PEMWA 2009* (IEEE, 2009), pp. 1–7.
[6]T. Lewis, A. von Jouanne, and T. Brekken, "Wave energy converter with wideband power absorption," in *Energy Conversion Congress and Exposition (ECCE), 2011* (IEEE, 2011), pp. 3844–3851.
[7]E. Tedeschi and M. Molinas, "Impact of control strategies on the rating of electric power take off for wave energy conversion," in *2010 IEEE International Symposium on Industrial Electronics (ISIE)* (2010), pp. 2406–2411.
[8]G. Li, G. Weiss, M. Mueller, S. Townley, and M. R. Belmont, "Wave energy converter control by wave prediction and dynamic programming," Renewable Energy **48**, 392–403 (2012).
[9]E. Tedeschi, M. Carraro, M. Molinas, and P. Mattavelli, "Effect of control strategies and power take-off efficiency on the power capture from sea waves," IEEE Trans. Energy Convers. **26**, 1088–1098 (2011).
[10]M. Eriksson, J. Isberg, and M. Leijon, "Theory and experiment on an elastically moored cylindrical buoy," IEEE J. Oceanic Eng. **31**, 959–963 (2006).
[11]J. Falnes, *Ocean Waves and Oscillating Systems. Linear Interaction Including Wave-Energy Extraction* (Cambridge University Press, 2004).
[12]R. Waters, M. Stalberg, O. Danielsson, O. Svensson, S. Gustafsson, E. Strömstedt, M. Eriksson, J. Sundberg, and M. Leijon, "Experimental results from sea trials of an offshore wave energy system," Appl. Phys. Lett. **90**, 034105–3 (2007).
[13]M. Leijon, C. Boström, O. Danielsson, S. Gustafsson, K. Haikonen, O. Langhamer, E. Strömstedt, M. Ståberg, J. Sundberg, O. Svensson, S. Tyrberg, and R. Waters, "Wave energy from the north sea: Experiences from the lysekil research site," Surv. Geophys. **29**, 221–240 (2008).
[14]See "http://www.wamit.com/" for WAMIT.
[15]R. Waters, M. Rahm, M. Eriksson, O. Svensson, E. Strömstedt, C. Boström, J. Sundberg, and M. Leijon, "Ocean wave energy absorption in response to wave period and amplitude—Offshore experiments on a wave energy converter," IET Renewable Power Gener. **5**, 465–469 (2011).
[16]M. Eriksson, R. Waters, O. Svensson, J. Isberg, and M. Leijon, "Wave power absorption: Experiments in open sea and simulation," J. Appl. Phys. **102**, 084910 (2007).
[17]R. Waters, J. Engström, J. Isberg, and M. Leijon, "Wave climate off the swedish west coast," Renewable Energy **34**, 1600–1606 (2009).